JOURNAL OF AIRCRAFT
Vol. 36, No. 6, November–December 1999

Multipoint Inverse Design Method for Transonic Wings

Hyoung-Jin Kim,* Chongam Kim,† and Oh-Hyun Rho‡
Seoul National University, Seoul 151-742, Republic of Korea

A new multipoint inverse design method to improve aerodynamic performance of transonic transport wings at off-design conditions is demonstrated. We minimized weighted averages of the residuals that are differences between computed and target pressures at two design points. Target pressure distributions are optimized using a genetic algorithm. It was found that characteristics of single-point design wings were transferred to dual-point design wings proportionally to weighting factors. Through the dual-point design procedure, off-design performance of a single-point design wing is improved while preserving good performance at the primary design point. The present dual-point design procedure requires about 12 times the computational cost of a flow solver and is, therefore, very efficient for the multipoint design of transonic wings.

Nomenclature

A	= normalized wing section area (area/c^2)
C_L, C_{Dw}	= wing lift and wave drag coefficient
C_{pt}, C_{pc}	= target and computed pressure coefficient
c	= wing section chord length
t/c	= maximum thickness-to-chordratio of a wing section
η	= semispan fraction, $2y/b$
$\Lambda_{1/2}$	= sweep angle of $\frac{1}{2}$ chord line

Subscript

0	= value of the baseline wing

Introduction

WITH the advances in computational fluid dynamics, computational design methods in the aerodynamic design of aircraft components are more important than ever before. Computational methods in aerodynamic design can be categorized into two classes: direct numerical optimization methods and inverse design methods. Inverse design methods are much faster and more efficient than direct numerical optimization methods. However, there are several issues to be resolved in inverse design methods.

First, inverse design methods require aerodynamic designers to specify a target pressure distribution producing improved aerodynamic performances and satisfying structural and manufactural constraints. Although experienced aerodynamicists can identify desirable flow characteristics, for example, reduced shock strength and/or elimination of flow separation, it is not a trivial task to develop a target pressure distribution that will provide these benefits while maintaining other aerodynamic constraints such as lift and pitching moment. To overcome this defect, several researchers have been investigating the numerical optimization of the target pressure for inverse designs of transonic airfoils[1–3] and wings.[4]

Van Egmond[1] developed a target pressure optimization method and applied it to transonic and subsonic airfoil design cases. Aerodynamic shape functions were defined for a parameterization of the pressure distribution. He pointed out that the target pressure optimization problem is strongly nonlinear and exhibits discontinuous derivatives for the objective as well as constraint functions. This motivated the use of genetic algorithms (GA) in target pressure optimization problems. Obayashi and Takanashi[2] applied a GA to the target pressure optimization for transonic and subsonic wing section designs. They used the B-spline interpolation method for a parameterization of the target pressure distribution. Kim and Rho[3,4] also applied a GA for the target pressure optimization for transonic airfoils[3] and wings.[4] They considered three-dimensional features such as wing loading distribution and a shock sweep angle or isobar line sweep angles for a successful design of transonic wings.[4]

Second, inverse design methods are basically single-point design methods because the target pressure distribution will be matched at a given design condition. This may cause troubles in applying inverse methods to multipoint design problems. The single-point design approach does not guarantee good performance at off-design conditions,[3–5] and thus multipoint designs are essential for better aerodynamic performances under wider flight conditions.

Direct optimization methods have a strong point over inverse methods in the versatility of performing multipoint design problems. However, direct optimization methods require too much computational time for practical multipoint design[5] compared with inverse methods.[6] Recently, an adjoint method that requires much less computational time to calculate design sensitivities compared with other direct optimization methods was applied to a multipoint transonic wing design of a business jet configuration.[7]

Unlike direct optimization methods, it is not so straightforward to apply an inverse method to multipoint design problems, and some manipulations are needed to devise purely inverse design methods. Mineck et al.[6] applied an inverse design method to dual-point designs of transonic airfoils. They used two procedures: airfoil shape averaging and target pressure averaging, with an assumption that aerodynamic properties vary linearly with the weighting factor of airfoil shape averaging. It was found that the former procedure worked better for the specified design problem.

Kim and Rho[3] applied a hybrid inverse optimization method[8] to the multipoint design of transonic airfoils. A new objective function is defined as a weighted average of residuals that are differences between computed and target pressures at both design conditions, and the function is minimized by an optimization technique. It was also shown that a dual-point design airfoil minimizing the weighted-average of residuals demonstrates better performances than those obtained by shape averaging of single-point design airfoils at design conditions. A similar concept was also applied to the rotor blade design in forward flight condition by Tapia et al.[9]

The present paper describes a new dual-point design procedure for transonic wings using an inverse design method. Target pressures are optimized at both design conditions by a target pressure optimization code[4] with a GA. A wing geometry is then obtained that minimizes

Received 7 July 1998; revision received 15 March 1999; accepted for publication 20 May 1999.

*Graduate Research Assistant, Department of Aerospace Engineering; hyoungj@gong.snu.ac.kr. Member AIAA.

†Assistant Professor, Department of Aerospace Engineering. Member AIAA.

‡Professor, Department of Aerospace Engineering. Senior Member AIAA.

the weight-averaged residual and satisfies geometric constraints through the hybrid inverse optimization method.

Following this introduction, a brief review of the flow solver used is given. The multipoint inverse design procedure and target pressure optimization method are presented in detail, followed by two examples of transonic transport wing design. Based on the computed results, we draw conclusions.

Flow Analysis

A three-dimensional Navier–Stokes solver developed and validated in Refs. 4 and 10 is used for the flow analysis. Three-dimensional Reynolds-averaged thin-layer Navier–Stokes equations in generalized coordinates are used in the conservation form based on a cell-centered finite volume approach. Roe's flux difference splitting scheme is adopted for the space discretization, and the MUSCL approach with a Koren flux limiter is employed to obtain a third-order accuracy. Yoon and Jameson's Lower–Upper Symmetric Gauss–Seidel method is used for the time integration. Turbulence effects are considered using the Baldwin–Lomax model with a relaxation technique.

We used a C–O type of grid system around a wing with 135 points in the streamwise direction, 41 points in the normal direction, and 30 points in the spanwise direction. Although somewhat coarse grids are used, it is shown in Ref. 4 that this grid system captures accurate surface pressure distributions and gives comparable aerodynamic coefficients with the results of fine grids.

The residual of the flow solver is reduced by three orders of magnitude from the freestream value in the inverse design procedures and by four orders to obtain the aerodynamic coefficients of the final wings.

Multipoint Inverse Design Procedure

We used a three-dimensional inverse design code[4] that adopts the following Modified Garabedian–Mcfadden (MGM) equation[11] to solve an inverse problem at chordwise wing sections:

$$F_0\Delta z + F_1\Delta z_x + F_2\Delta z_{xx} = R, \qquad (R = C_{pt} - C_{pc}) \quad (1)$$

where R is the residual that is the difference between the target and computed pressure, and coefficients F_0, F_1, and F_2 are nonnegative constants chosen to provide a stable iterative process. In this study, the coefficients of the derivative terms are determined by local flow conditions on the body surface. If the local flow is subsonic, the coefficient F_1 of the first derivative term is set to zero. Otherwise, the coefficient F_2 of the second derivative term is set to zero. In either case only two out of the three terms on the left-hand side remain. Then the MGM method becomes similar to the direct iterative surface curvature method.[12] The switching Mach number was set to $1.1/\sin\Lambda_{1/2}$ $(= 1.17)$ by applying the simple sweep theory. The MGM equation is then solved using a finite difference scheme. A discretized MGM equation forms a tridiagonal system and can be written as

$$[M]\{\overline{\Delta z}\} = \{R\} \quad (2)$$

The detailed expressions for elements of matrix $[M]$ are given by Malone et al.[11]

An objective function is defined as follows to solve Eq. (2) with an optimization technique:

$$F(\overline{\Delta z}) = \tfrac{1}{2}|[M]\{\overline{\Delta z}\} - \{R\}|^2 \quad (3)$$

An exterior penalty function method is used to specify geometric constraints, and a conjugate gradient method[13] is utilized to minimize the objective function of Eq. (3). The computational time required to calculate the objective function and its derivative is negligible compared with the time required by the flow solver.

The preceding method, developed by Santos and Sankar,[8] is referred to as the hybrid inverse optimization method because it solves an inverse design problem with an optimization technique.

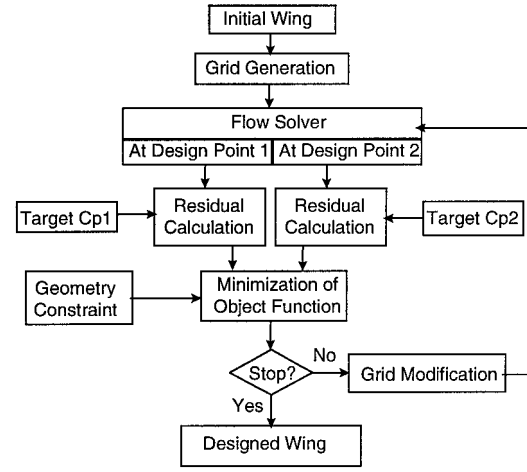

Fig. 1 Flowchart of dual-point inverse wing design.

To perform a dual-point design, the following objective function, which averages the two objective functions at two design points as defined in Ref. 3, is to be minimized:

$$F(\overline{\Delta z}) = (w/2)|[M_1]\{\overline{\Delta z}\} - \{R_1\}|^2 + [(1-w)/2]|[M_2]\{\overline{\Delta z}\} - \{R_2\}|^2 \quad (4)$$

where w is a weighting factor, which can vary from 0 to 1. A weighting factor of 1 corresponds to a single-point design at design condition 1, and a weighting factor of 0 corresponds to a single-point design at design condition 2.

Figure 1 is the flowchart of the dual-point transonic wing design procedure. Target pressures are optimized with a GA for given two flow conditions and constraints. Vertical displacements of design section grid points are then obtained that minimize the objective function [Eq. (4)] and satisfy geometric constraints. Design sections are updated and fitted to a 10th-order polynomial to produce a smooth section shape with continuous first and second derivatives. Wing section shapes other than the design sections are interpolated from the design sections by the C-spline method inboard and by the linear interpolation outboard. Because drastic changes on the wing section geometry are not expected, the grid points around the wing are modified algebraically. This design cycle is repeated until geometric modifications are sufficiently small.

One can extend the present dual-point design procedure to a more general multipoint design problem by simply adding more residual terms in the objective function of Eq. (4). Because the number of weighting factor increases in that case, one should be careful in selecting a combination of weighting factors.

Although we adopted a target pressure optimization approach and an inverse design method in this study, one may use a surface pressure distribution of a single-point design wing by a direct optimization method as a target pressure distribution. The weighted average of residuals can also be minimized by a direct optimization technique.

Target Pressure Optimization

We utilized a target pressure optimization code developed by the authors[4] for the optimization of target pressure distributions at given design conditions. Figure 2 shows a characteristic surface pressure distribution defined by eight control points for a typical transonic wing section. Aerodynamic shape functions are used to interpolate between these points. Locations, the local Mach numbers of characteristic points, and coefficients of shape functions are used as design variables. We employed 15 design parameters for a design section. Because three design sections are selected in this study, the total number of design variables is 45.

The target pressure can be generated at each design section of a wing in a two-dimensional manner. However, three-dimensional characteristics, such as spanwise wing loading distribution and shock sweep angles or isobar line sweep angles, are considered

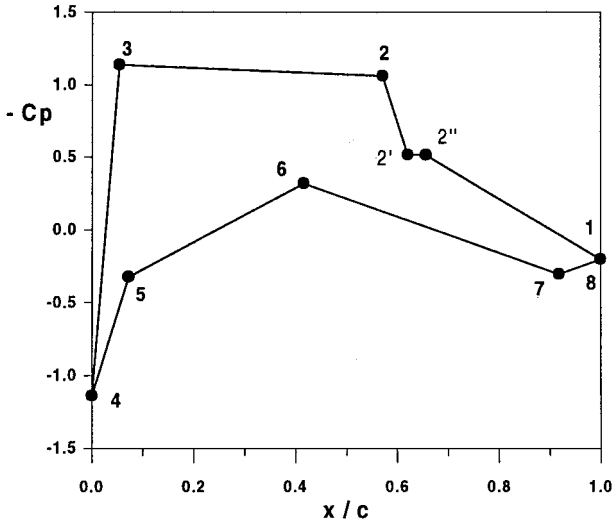

Fig. 2 Schematic representation of target pressure distribution.

in the target pressure optimization code for a successful design of transonic wings.

The objective of the target pressure optimization in this study is to obtain a target pressure distribution that has a minimum wave drag, while the lift and the section maximum thickness remain almost the same as the baseline wing. The wave drag can be minimized by decreasing shock strength and by maximizing a shock sweep angle. The spanwise wing loading is specified as an elliptic distribution to reduce the induced drag. The optimization problem is then defined as follows:

$$\text{Minimize} \qquad C_{Dw} \tag{5}$$

subject to 1) elliptic wing loading distribution, 2) $t_0/c - 0.001 \leq t/c \leq t_0/c + 0.001$, and 3) $\mathrm{d}C_p/\mathrm{d}(x/c) \leq 2.3$.

The third constraint on the pressure gradient is specified to avoid flow separation at pressure recovery regions. Some other constraints were also imposed to obtain a reasonable pressure distribution.

In the present study on dual-point inverse designs, one of major concerns is to maintain the consistency of the two target pressure distributions optimized at two different design conditions. Inconsistency of the two target pressure distributions can usually occur around the leading edge and on the lower surface of a wing section. We alleviated this problem by specifying additional constraints that the pressure distribution on the lower surface and around the leading edge should be similar to that of the baseline wing.

All the constraints were included in the objective function as penalty function terms multiplied by proper weighting factors. To minimize the objective function, we utilized the Genocop code,[14] which adopts a GA. Readers are referred to Ref. 4 for further details of the target pressure optimization.

Results and Discussion

The baseline wing in this design study is the W7850 wing that was designed in Ref. 4 with $M_\infty = 0.78$, $C_L = 0.50$, and $Re = 7 \times 10^6$ based on the root chord length. The leading-edge sweep angle of the baseline wing is 27 deg, and the aspect ratio is 8.49. Chord length ratio of wing tip to root is 0.266, and chord length ratio of wing trailing-edge kink position to root is 0.58. Thickness-to-chord ratio of the section airfoil is 15% at the root and 11% at the kink and tip. The twist angle is 4 deg. The planform and twist angle of the baseline wing are kept constant in the design process. Three design sections are selected at $\eta = 0.057$, 0.343, and 0.918. The second design section is at the kink position.

In the following design examples, design condition 1 is $M_\infty = 0.78$ and $C_L = 0.50$ with $Re = 7 \times 10^6$ based on the root chord length. Design condition 2 is selected as a higher Mach number or a higher lift coefficient than the first design condition. Although the aerodynamic performance of the baseline wing is very high at design condition 1, it rapidly decreases as the flow condition changes from design condition 1 to 2. The objective of the following design examples is to improve the performance of W7850 at design condition 2 while preserving its high performance at design condition 1. This objective can be interpreted as follows:

$$\text{Maximize} \qquad (L/D)_1$$

$$\text{subject to} \qquad K \equiv (L/D)_2 - 0.95(L/D)_1 \geq 0 \tag{6}$$

A small value of K means a rapid decrease of L/D value, whereas a larger K means a slow decrease as the flow condition changes from design condition 1 to 2.

Geometric constraints on design section areas are specified in the inverse design code to make the section areas of design wing similar to those of the baseline wing (W7850) as follows:

$$0.0900 \leq A_{\mathrm{ds}1} \leq 0.0920, \qquad 0.0708 \leq A_{\mathrm{ds}2} \leq 0.0720$$

$$0.0708 \leq A_{\mathrm{ds}3} \leq 0.0720 \tag{7}$$

Other geometric constraints such as maximum thickness and nose radius can also be imposed in the inverse design code. However, such constraints were specified only in the target pressure generation level and were not specified in the inverse design code explicitly.

Design Example I (Mach Design)

The freestream Mach number M_∞ of design condition 2 is increased to 0.80 with other conditions unchanged from those of design condition 1. Target pressure distributions are optimized by a GA with 200 population and a maximum generation number of 1500.

With the optimized target pressures at the design sections, a single-point design is conducted at design condition 2 to obtain W8050, which represents a wing designed at $M_\infty = 0.80$ and $C_L = 0.50$. Dual-point designs are then conducted for three weighting factors: 0.25, 0.50, and 0.75. In both single- and dual-point design runs, the inverse design routine was stopped after 10 iterations.

It takes about 1.5 times the computational cost of a flow analysis to conduct a single-point design, and about 3 times the computational cost of a flow analysis to obtain the final wing geometry for each of the three chosen weighting factors.[4] Hence, it requires about 12 times the cost of a flow solver to conduct two single-point designs and three dual-point designs. This implies that the present approach is very efficient compared with a direct optimization method[5] in which more than 60 flow analyses were required for a dual-point design of a two-dimensional transonic airfoil with 16 design variables.

The aerodynamic performances of the design wings are presented in Table 1. The value of K increases as the weighting factor decreases, meaning that the lift-to-drag ratio decreases more slowly for smaller weighting factors as the Mach number increases. This shows that the characteristics of the single-point design wings are transferred to the dual-point design wings proportionally to the weighting factors.

In this example the design wing with a weighting factor of 0.75 yields the optimum solution among the five wings for the optimization problem of Eq. (6) because it has a positive value of K and the largest value of $(L/D)_1$. If more weighting factors are introduced, one would have more chances to find a better wing at the cost of computational time.

Table 2 compares section areas and maximum thickness ratios of the design wings. Area constraints were imposed in the inverse

Table 1 Mach design results ($M_{\infty 1} = 0.78$, $M_{\infty 2} = 0.80$, $C_L = 0.50$)

w	$(L/D)_1$	$(L/D)_2$	K[a]
1.0 (W7850)	23.89	21.99	−0.7055
0.75	23.89	22.77	0.0745
0.50	23.63	23.03	0.5815
0.25	23.65	23.13	0.6625
0.0 (W8050)	23.76	23.30	0.7280

[a] $K[\equiv (L/D)_2 - 0.95(L/D)_1]$.

Table 2 Mach design: section areas and maximum thickness ratios

	A			$(t/c) \times 100$, %		
Wing	ds1[a]	ds2	ds3	ds1	ds2	ds3
W7850	0.0920	0.0720	0.0720	13.4	10.9	11.1
W8050	0.0899	0.0720	0.0717	13.0	10.9	10.8
$w = 0.75$	0.0910	0.0721	0.0720	13.3	10.9	11.0

[a]Design section, ds.

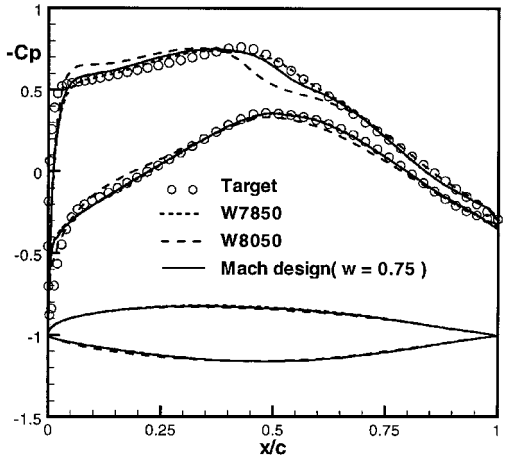

Design section 1 (η = 0.057)

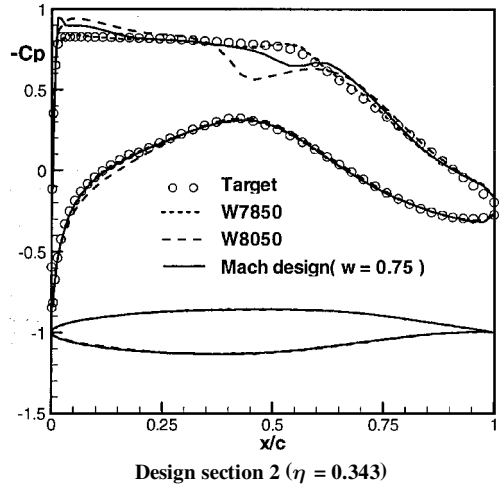

Design section 2 (η = 0.343)

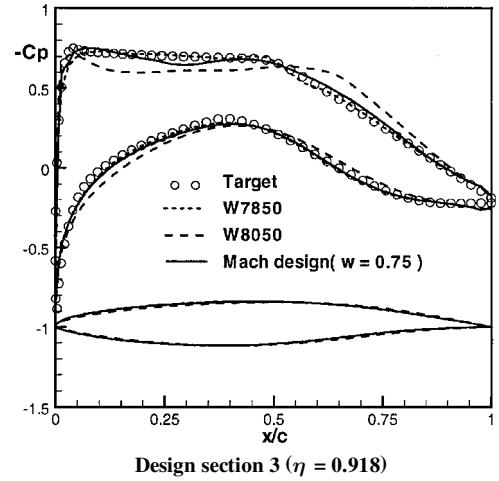

Design section 3 (η = 0.918)

Fig. 3 Mach design result: Surface pressure and section airfoil shape at design condition 1 (M_∞ = 0.78 and C_L = 0.50).

design code, whereas the maximum thickness constraints were implicitly specified in the target pressure distributions. Because the area constraints are closely related to the maximum thickness constraints, one can hardly satisfy the area constraints if the thickness constraints are not properly imposed in the target pressure distributions. All the design sections satisfy the area constraints of Eq. (7). The maximum thickness ratios of the design wings are successfully controlled such that they are similar to those of the baseline wing (W7850).

Figure 3 shows pressure distributions at design condition 1 and wing section shapes at each design section. W8050 has a weak shock at design section 2, whereas the Mach design wing has similar pressure distributions to W7850. Pressure distributions at design condition 2 are presented in Fig. 4. W8050 has almost identical pressure distributions with target pressures. W7850 yields a strong shock on the upper surface, which is reduced by the Mach design.

Overall feature of the design results can be seen in Fig. 5. W8050 has a smaller shock sweep angle than the other two wings at design

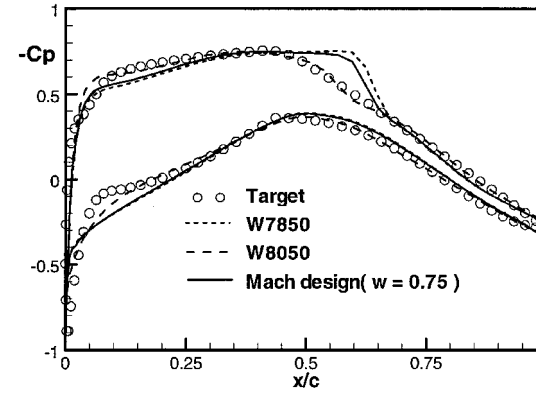

Design section 1 (η = 0.057)

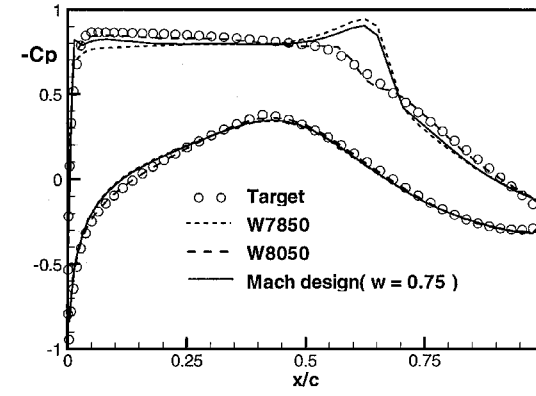

Design section 2 (η = 0.343)

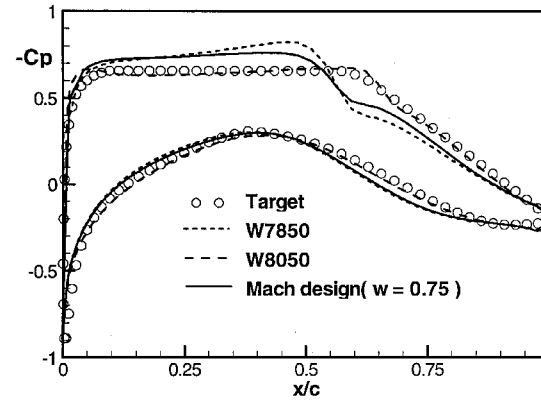

Design section 3 (η = 0.918)

Fig. 4 Mach design result: surface pressure at design condition 2 (M_∞ = 0.80 and C_L = 0.50).

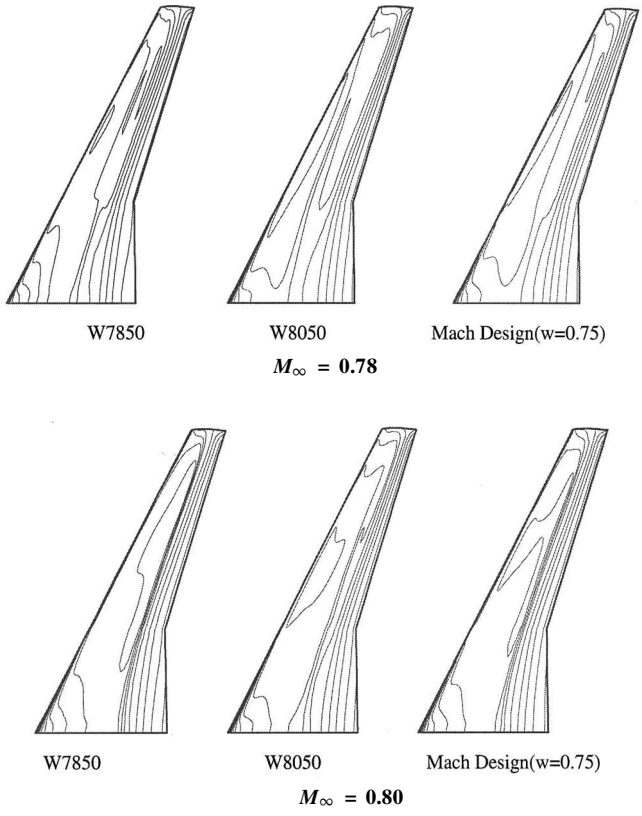

Fig. 5 Mach design result: upper surface pressure contours at C_L = 0.50.

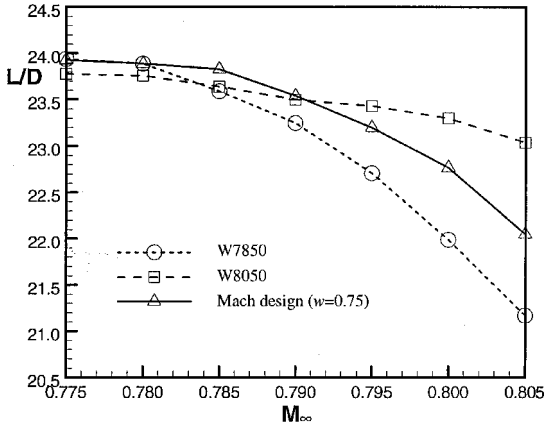

Fig. 6 M_∞ vs L/D curves at C_L = 0.50.

point 1 ($M_\infty = 0.78$). On the other hand, W7850 has a strong shock, and the Mach design wing has a weaker shock than W7850 at design point 2.

Off-design performances of design wings are shown in Fig. 6. Compared to W7850, the lift-to-drag ratio of the Mach design wing is substantially improved at the Mach numbers higher than 0.78.

Design Example II (α Design)

The objective of the second design example is to improve an off-design performance of W7850 when the lift coefficient is increased by 0.10. The design condition 1 is the same as in design example I. Flow conditions at design condition 2 are $C_L = 0.60$, with other conditions fixed. The incidence angle α is increased to obtain a lift coefficient of 0.60.

The target pressure distributions of both design conditions at three design sections are optimized with the same objectives and constraints as in the first design example. The GA is also run with the same number of population and maximum generation.

With optimized target pressure distributions, the dual-point inverse design code was run for three weighting factors: 0.25, 0.50, and 0.75. The aerodynamic performance of design wings for these weighting factors are presented in Table 3. As in the Mach design case, the value of K increases as the weighing factor decreases, which indicates again that the lift-to-drag ratio decreases more slowly for smaller weighting factors as the lift coefficient goes up.

In this case the optimum wing for the optimization problem of Eq. (6) among the five wings is a design wing with a weighting factor of 0.75, which has a positive value of K and the largest value

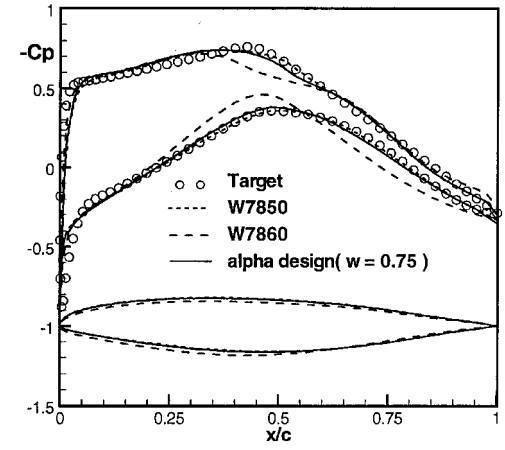

Design section 1 (η = 0.057)

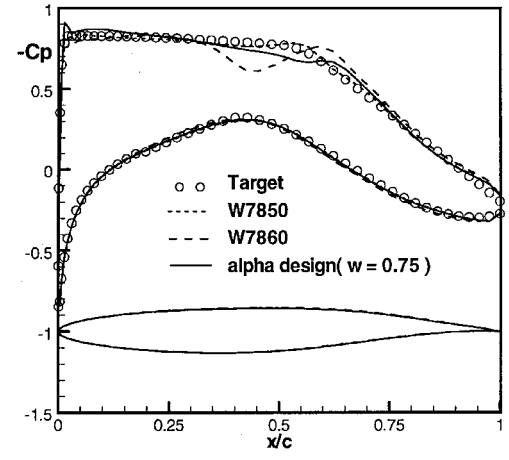

Design section 2 (η = 0.343)

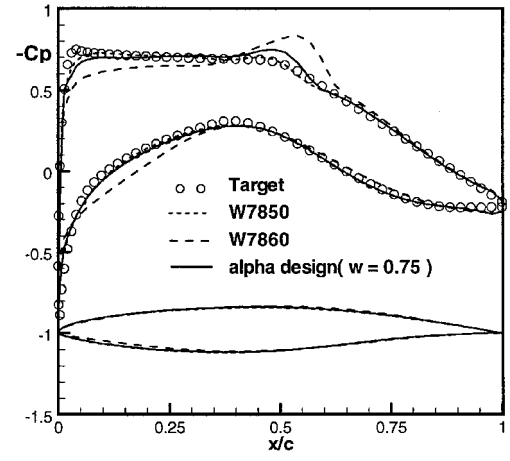

Design section 3 (η = 0.918)

Fig. 7 Angle α design result: surface pressure and section airfoil shape at design condition 1 (M_∞ = 0.78 and C_L = 0.50).

Table 3 Angle α design results ($M_\infty = 0.78$, $C_{L1} = 0.50$, $C_{L2} = 0.60$)

w	$(L/D)_1$	$(L/D)_2$	K
1.0 (W7850)	23.89	22.48	−0.2155
0.75	23.89	22.91	0.2145
0.50	23.66	22.70	0.2230
0.25	23.79	22.87	0.2695
0.0 (W7860)	23.73	23.10	0.5565

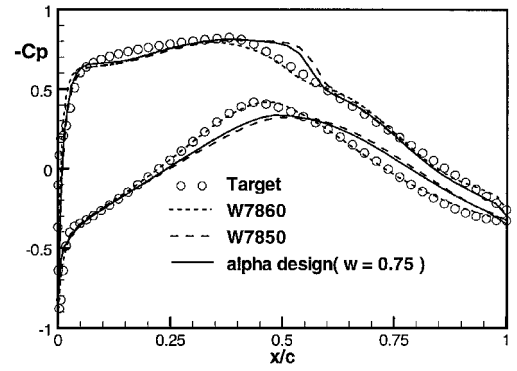

Design section 1 ($\eta = 0.057$)

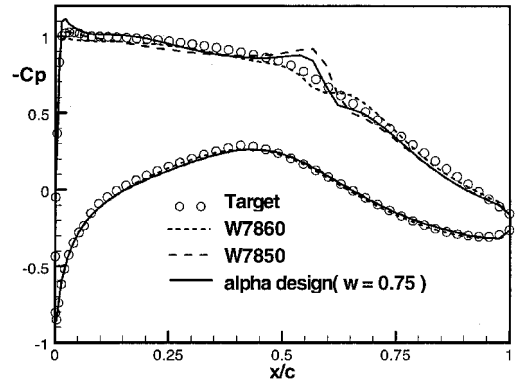

Design section 2 ($\eta = 0.343$)

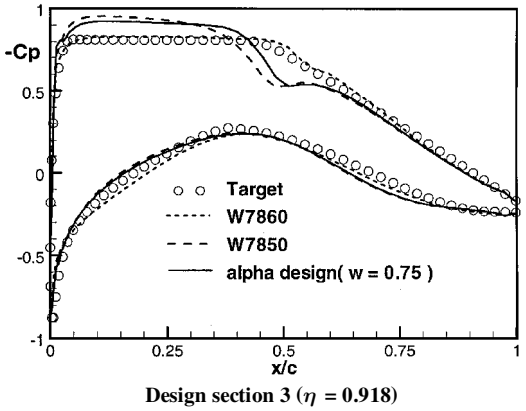

Design section 3 ($\eta = 0.918$)

Fig. 8 Angle α design result: surface pressure at design condition 2 ($M_\infty = 0.78$ and $C_L = 0.60$).

Table 4 Angle α design: section areas and maximum thickness ratios

	A			$(t/c) \times 100$; %		
Wing	ds1[a]	ds2	ds3	ds1	ds2	ds3
W7850	0.0920	0.0720	0.0720	13.4	10.9	11.1
W7860	0.0900	0.0720	0.0719	13.6	10.9	11.1
$w = 0.75$	0.0918	0.0717	0.0728	13.5	10.8	11.2

[a]Design section, ds.

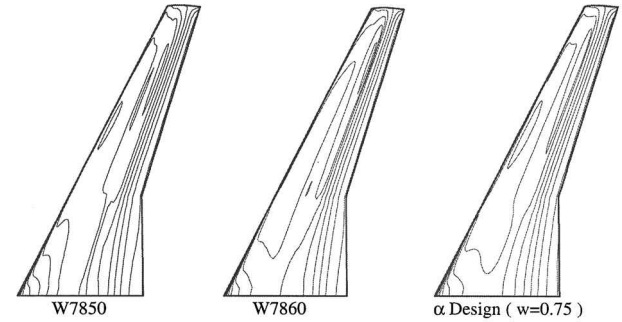

$C_L = 0.50$

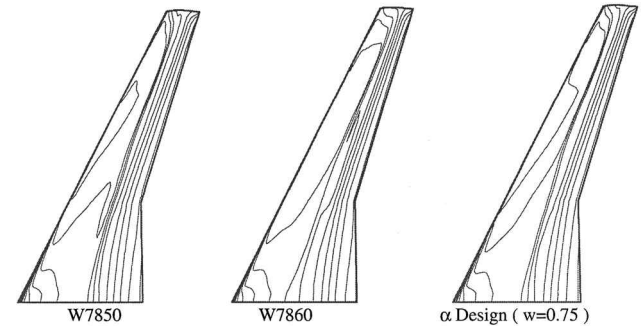

$C_L = 0.60$

Fig. 9 Angle α design result: upper surface pressure contours at $M_\infty = 0.78$.

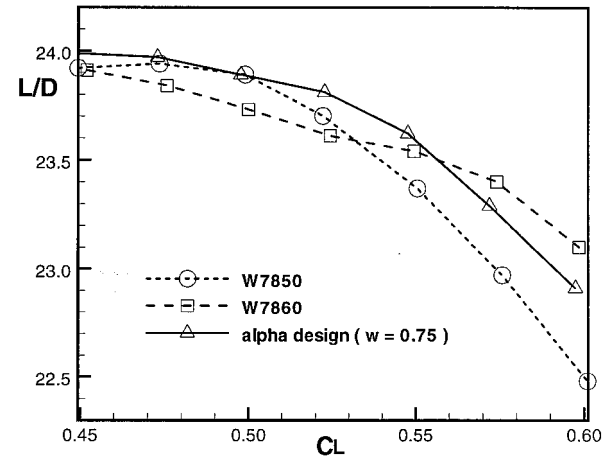

Fig. 10 C_L vs L/D curves at $M_\infty = 0.78$.

of $(L/D)_1$. If the objective is to maximize to the summation of the lift-to-drag ratio at both design points, the optimum wing here would be W7860, which is the single-point design wing at design condition 2.

Table 4 presents section areas and maximum thickness ratios of the design wings. All the wing sections satisfy the area constraints of Eq. (7) except the third design section of the dual-point design ($w = 0.75$) wing. This might be caused by the 10th-orderpolynomial used for fitting the design section contours. As in the Mach design example, the maximum thickness ratios of the design wings are successfully constrained in a way that they are similar to those of the baseline wing (W7850).

Figure 7 shows the pressure distributions at design condition 1 and the wing section shapes at each design section. The secondary point design wing (W7860) has a stronger shock wave compared to the other two wings. Pressure distributions at design condition 2 are presented in Fig. 8. W7860 renders almost identical pressure distributions with the target pressures. W7850 has a strong shock, whereas the shock strength is much reduced in the α design wing.

Figure 9 shows upper surface pressure contours of W7850, W7860, and the α design wing at both design conditions. W7860

exhibits a stronger shock outboard than the other two wings at design point 1 ($C_L = 0.5$). At design point 2 ($C_L = 0.6$), a strong shock occurs on the upper surface of W7850, but the α design wing has a weaker shock than W7850.

C_L vs L/D curves are also shown in Fig. 10. The lift-to-drag ratios are increased from those of the baseline wing (W7850) by the α design at lift coefficients other than 0.50.

We did not compare the dual-point design wings with the wing by shape averaging proposed by Mineck et al.[6] explicitly. However, it is noted that the present design wings would show better performances than a wing by shape averaging because the dual-point design wing shows more than average performance of the two single-point design wings.

Conclusions

We performed a multipoint inverse design study of transonic wings. A target pressure optimization code with a GA was used for the specification of target pressure distributions at each design condition. A weighted average of residuals at two design points is minimized by the conjugate gradient method. Characteristics of the single-point design wings are transferred to the dual-point design wings proportionally to the weighting factors. The dual-point design wings show better performance than the single-point design wings at the secondary design condition, while maintaining high performance at the primary design condition. The computational cost required in the dual-point design procedure with three weighting factors is about 12 times that of a flow solver. Therefore, poor performances of single-point designed wings at off-design conditions can be improved very efficiently with the present dual-point design method.

References

[1]van Egmond, J. A., "Numerical Optimization of Target Pressure Distributions for Subsonic and Transonic Airfoil Design," *Computational Methods for Aerodynamic Design (Inverse) and Optimization*, AGARD 463, Ref. 17, March 1990.

[2]Obayashi, S., and Takanashi, S., "Genetic Optimization of Target Pressure Distributions for Inverse Design Methods," *AIAA Journal*, Vol. 34, No. 5, 1996, pp. 881–886.

[3]Kim, H. J., and Rho, O. H., "Dual-Point Design of Transonic Airfoils Using the Hybrid Inverse Optimization Method," *Journal of Aircraft*, Vol. 34, No. 5, 1997, pp. 612–618.

[4]Kim, H. J., and Rho, O. H., "Aerodynamic Design of Transonic Wing Using the Target Pressure Optimization Approach," *Journal of Aircraft*, Vol. 35, No. 5, 1998, pp. 671–677.

[5]Hager, J. O., Eyi, S., and Lee, K. D., "Two-Point Transonic Airfoil Design Using Optimization for Improved Off-Design Performance," *Journal of Aircraft*, Vol. 31, No. 5, 1994, pp. 1143–1147.

[6]Mineck, R. E., Campbell, R. L., and Allison, D. O., "Application of Two Procedures for Dual-Point Design of Transonic Airfoils," NASA TP-3466, Sept. 1994.

[7]Reuther, J., Jameson, A., Alonso, J. J., Rimlinger, M. J., and Saunders, D., "Constrained Multipoint Aerodynamic Shape Optimization Using an Adjoint Formulation and Parallel Computers," AIAA Paper 97-0103, Jan. 1997.

[8]Santos, L. C., and Sankar, L. N., "A Hybrid Inverse Optimization Method for the Aerodynamic Design of Lifting Surfaces," AIAA Paper 94-1895, June 1994.

[9]Tapia, F., Sankar, L. N., and Shrage, D. P., "An Inverse Aerodynamic Design Method for Rotor Blades," *Journal of the American Helicopter Society*, Vol. 42, No. 4, 1997, pp. 321–326.

[10]Hwang, S. W., "Numerical Analysis of Unsteady Supersonic Flow over Double Cavity," Ph.D. Dissertation, Dept. of Aerospace Engineering, Seoul National Univ., Seoul, Korea, Feb. 1996.

[11]Malone, J. B., Narramore, J. C., and Sankar, L. N., "Airfoil Design Method Using the Navier–Stokes Equations," *Journal of Aircraft*, Vol. 28, No. 3, 1991, pp. 216–224.

[12]Campbell, R. L., and Smith, L. A., "A Hybrid Algorithm for Transonic Airfoil and Wing Design," AIAA Paper 87-2552, June 1987.

[13]Press, W. H., Teukolsky, S. A., Vetterling, W. T., and Flannery, B. P., "Numerical Recipes in FORTRAN," 2nd ed., Cambridge Univ. Press, Cambridge, England, UK, 1992, pp 413–418.

[14]Michalewicz, Z., *Genetic Algorithms + Data Structures = Evolution Programs*, Springer–Verlag, New York, 1992, Chap. 7, pp. 121–154.